

Robust optimal control using dynamic programming and guaranteed Euler’s method

Jawher Jerray¹, Laurent Fribourg², and Étienne André³[0000–0001–8473–9555]

¹ Université Sorbonne Paris Nord, LIPN, CNRS, UMR 7030, F-93430, Villetaneuse, France

² Université Paris-Saclay, LSV, CNRS, ENS Paris-Saclay

³ Université de Lorraine, CNRS, Inria, LORIA, F-54000 Nancy, France
jerray@lipn.univ-paris13.fr

Abstract. Set-based integration methods allow to prove properties of differential systems, which take into account bounded disturbances. The systems (either time-discrete, time-continuous or hybrid) satisfying such properties are said to be “robust”. In the context of optimal control synthesis, the set-based methods are generally extensions of numerical optimal methods of two classes: first, methods based on convex optimization; second, methods based on the dynamic programming principle. Heymann et al. have recently shown that, for certain systems of low dimension, the second numerical method can give better solutions than the first one. They have built a solver (Bocop) that implements both numerical methods. We show in this paper that a set-based extension of a method of the second class which uses a guaranteed Euler integration method, allows us to find such good solutions. Besides, these solutions enjoy the property of robustness against uncertainties on initial conditions and bounded disturbances. We demonstrate the practical interest of our method on an example taken from the numerical Bocop solver. We also give a variant of our method, inspired by the method of Model Predictive Control, that allows us to find more efficiently an optimal control at the price of losing robustness.

1 Introduction

Given a differential system with input of the form $\dot{y}(t) = f(y(t), \mathbf{u}(t))$ and an initial condition $y(0) = y_0$, the calculation of a control $\mathbf{u}(\cdot)$ that minimizes a given cost function (*optimal control*) rarely has an analytical solution, and numerical methods must be used to obtain approximate solutions. Among these numerical methods, there are 3 main classes:

1. methods that reduce the problem to a *convex optimization* problem, which are very much in demand since the adaptation of interior point methods by Nesterov and Nemirovskii [NN94], and which are notably used in receding horizon methods, also called Model Predictive Control (MPC) [May14];

2. methods based on the resolution of an Hamilton-Jacobi-Bellman (HJB) equation (see, e.g., [FG99; SAF18]), using the *Dynamic Programming Principle* (DPP) [Bel57];
3. methods based on the *Pontryagin Maximum Principle* (PMP) [Kir70].

On the other hand, since the 1960s and the invention of Interval Arithmetic [Moo66], one has been looking for safe enclosures for the approximate values of ODEs computed by numerical methods. Therefore, extensions of numerical methods, called set-based (or symbolic) methods, have been used, which, instead of manipulating points, manipulate sets (typically real intervals or products of real intervals) in order to enclose the exact values. These methods of control synthesis are called “correct-by-design” or “guaranteed”. In addition to ensuring that a set (typically an interval) containing the exact solution is obtained at the end, set-based methods allow taking into account bounded disturbances. They are said to be “robust”. Since the beginning of interval arithmetic, these set-based methods have experienced a great development. The manipulated sets, originally products of real intervals [Moo66], have taken specialized convex forms such as polytopes [HK06], parallelotopes [Loh87], zonotopes [Gir05], spheres [Le +17b] or ellipsoids [Neu93]. In this context, numerical integration methods classically take set-based forms using extensions of Taylor’s methods (see, e.g., [ASB07; BH98; BM98; CAS12; Loh87; NJC99; NKS04]).

Numerical methods 1 and 2 of *optimal control* have themselves been subject to set-based extensions to take account of uncertainties (unlike method 3, which is very sensitive to initial conditions, and *a priori* unsuitable for set-based extensions). Extensions of numerical methods of class 1 are thus given in [MSR05; SA17a; SA17b; SKA18], while extensions of numerical methods of class 2 are given in [CF19a; CF19b; LTS99; MBT01; MT03; RR19]. These extensions have the respective advantages and disadvantages of their numerical counterparts. Set-based methods of class 1 are efficient (polynomial complexity in n -dimension of the problem, i.e., state vector dimension), but calculate *a priori* only *local* optimals. Set-based methods of class 2 compute global optimals, but undergo the “curse of dimensionality” (exponential complexity in the dimension M of the state space), and are limited to low dimensional problems.

Recently, in the numerical framework, Heymann et al. [Hey+18] have shown that, for certain problems, numerical methods of class 2 can give better solutions than numerical methods of class 1. They have built a numerical solver, called “Bocop”, that implements both classes of methods [Tea17], and have given a set of examples that allows to evaluate and compare them [BMG12]. We show in this paper that a set-based method of class 2 combining DPP and a guaranteed Euler integration method [CF19a], also allows us to compute approximate optimal solutions with good precision. Besides, these solutions enjoy the property of *robustness* against uncertainties on initial conditions and bounded disturbances. We demonstrate the practical interest of our method on an example taken from the Bocop solver. We also give a variant of our set-based method, inspired by the principle of Model Predictive Control [May14], that allows us to compute

approximate optimal solutions more quickly, at the cost of losing the robustness property.

Plan of the paper: In [Section 2](#), we explain the principle of our method of optimal control synthesis, and give the associated correctness results (convergence and robustness); we compare the results of our method with those obtained by the Bocop numeric solver on an example of Magnetic Resonance Imaging. In [Section 3](#), we give an efficient variant of our method inspired by the Model Predictive Control Approach but observe the loss of the robustness property. We conclude in [Section 4](#).

2 Robust optimal control

2.1 Explicit Euler time integration

We consider here a time discretization of time-step τ , and we suppose that the control law $\mathbf{u}(\cdot)$ is a *piecewise-constant* function, which takes its values on a *finite* set U , called “set of modes”. Given $u \in U$, let us consider the differential system controlled by u :

$$\frac{dy(t)}{dt} = f_u(y(t)).$$

where $f_u(y(t))$ stands for $f(\mathbf{u}(t), y(t))$ with $\mathbf{u}(t) = u$ for $t \in [0, \tau]$. We use Y_{t,y_0}^u to denote the exact continuous solution y of the system at time $t \in [0, \tau]$ under constant control u , with initial condition y_0 . This solution is approximated using the *explicit Euler* integration method. We use $\tilde{Y}_{t,y_0}^u \equiv y_0 + tf_u(y_0)$ to denote Euler’s approximate value of Y_{t,y_0}^u for $t \in [0, \tau]$.

Given a sequence of modes (or “pattern”) $\pi := u_1 \cdots u_k \in U^k$, we denote by Y_{t,y_0}^π the solution of the system under mode u_1 on $t \in [0, \tau]$ with initial condition y_0 , extended continuously with the solution of the system under mode u_2 on $t \in [\tau, 2\tau]$, and so on iteratively until mode u_k on $t \in [(k-1)\tau, k\tau]$. The control function $\mathbf{u}(\cdot)$ is thus piecewise constant with $\mathbf{u}(t) = u_n$ for $t \in [(n-1)\tau, n\tau)$, $1 \leq n \leq k$. Likewise, we use \tilde{Y}_{t,y_0}^π to denote Euler’s approximate value of Y_{t,y_0}^π for $t \in [0, k\tau)$ defined by $\tilde{Y}_{t,y_0}^{u_1 \cdots u_n} = \tilde{Y}_{t,y_0}^{u_1 \cdots u_{n-1}} + tf_{u_n}(\tilde{Y}_{t,y_0}^{u_1 \cdots u_{n-1}})$ for $t \in [0, \tau)$ and $2 \leq n \leq k$. The approximate solution \tilde{Y}_{t,y_0}^π is here a continuous piecewise linear function on $[0, k\tau)$ starting at y_0 .

2.2 Finite horizon control problems

The optimization task is to find a control pattern $\pi \in U^k$ which guarantees that all states in a given set $S = [0, 1]^M \subset \mathbb{R}^{M1}$ are steered at time $t_{end} = k\tau$ as closely as possible to an end state $y_{end} \in S$. Let us explain the principle of the

¹ We take here $S = [0, 1]^M$ for the sake of notation simplicity, but S can be any convex subset of \mathbb{R}^M .

method based on DPP and Euler integration method used in [CF19a; CF19b]. We consider the *cost function*: $J_k : S \times U^k \rightarrow \mathbb{R}_{\geq 0}$ defined by:

$$J_k(y, \pi) = \|Y_{k\tau, y}^\pi - y_{end}\|,$$

where $\|\cdot\|$ denotes the Euclidean norm in \mathbb{R}^{M2} .

We consider the *value function* $\mathbf{v}_k : S \rightarrow \mathbb{R}_{\geq 0}$ defined by:

$$\mathbf{v}_k(y) := \min_{\pi \in U^k} \{J_k(y, \pi)\} \equiv \min_{\pi \in U^k} \{\|Y_{k\tau, y}^\pi - y_{end}\|\}.$$

Given $k \in \mathbb{N}$ and $\tau \in \mathbb{R}_{>0}$, we consider the following *finite time horizon optimal control problem*: Find for each $y \in S$

– the *value* $\mathbf{v}_k(y)$, i.e.

$$\min_{\pi \in U^k} \{\|Y_{k\tau, y}^\pi - y_{end}\|\},$$

– and an *optimal pattern*:

$$\pi_k(y) := \arg \min_{\pi \in U^k} \{\|Y_{k\tau, y}^\pi - y_{end}\|\}.$$

In order to solve such optimal control problems, a classical “direct” method consists in *spatially discretizing* the state space $S = [0, 1]^M$ (i.e., the space of values of y). We consider here a uniform partition of S into a finite number N of cells of equal size: in our case, this means that interval $[0, 1]$ is divided into K subintervals of equal size, and $N = K^M$. A cell thus corresponds to a M -tuple of subintervals. The center of a cell corresponds to the M -tuple of the subinterval midpoints. The associated grid $\mathcal{X} \subset S$ is the set of centers of the cells of S . The center $z \in \mathcal{X}$ of a cell C is considered as the ε -*representative* of all the points of C . We suppose that the cell size is such that $\|y - z\| \leq \varepsilon$, for all $y \in C$ (i.e. $K \geq \sqrt{M}/2\varepsilon$).

We suppose that S is “controlled Euler-invariant” in the sense that, for all $y \in S$, there exists $u \in U$ such that $\tilde{Y}_{\tau, y}^u \in S$. We say that such u is *admissible* for y , and we denote by $Adm(y)$ the (non-empty) set of modes admissible for $y \in S$.

In this context, the method proceeds as follows (cf. [CF19a]): we consider the points of \mathcal{X} as the vertices of a finite oriented graph; there is a connection from $z \in \mathcal{X}$ to $z' \in \mathcal{X}$ if z' is the ε -representative of the Euler-based image $(z + \tau f_u(z))$ of z , for some $u \in U$. We then compute using dynamic programming the “path of length k with minimal cost” starting at z : such a path is a sequence of $k + 1$ connected points $z = z_k = z_{k-1} = \dots = z_1$ of \mathcal{X} which minimizes the distance $\|z_1 - y_{end}\|$. This procedure allows us to compute a pattern $\pi_k^\varepsilon(z)$ of length k , which approximates the optimal pattern $\pi_k(y)$.

Definition 1. *The function $next^u : \mathcal{X} \rightarrow \mathcal{X}$ is defined by:*

² We consider here the special case where the cost function is only made of a “terminal” subcost. The method extends to more general cost functions. Details will be given in the extended version of this paper.

- if $u \in \text{Adm}(z)$, then: $\text{next}^u(z) = z'$, where $z' \in \mathcal{X} \subset S$ is the ε -representative of $\tilde{Y}_{\tau,z}^u$.
- otherwise (i.e., $\tilde{X}_{\tau,z}^u \notin S$): $\text{next}^u(z) = \perp$.

Definition 2. For all point $z \in \mathcal{X}$, the spatially discrete value function $\mathbf{v}_k^\varepsilon : \mathcal{X} \rightarrow \mathbb{R}_{\geq 0}$ is defined by:

- for $k = 0$, $\mathbf{v}_k^\varepsilon(z) = \|z - y_{\text{end}}\|$,
- for $k \geq 1$, $\mathbf{v}_k^\varepsilon(z) = \min_{u \in \text{Adm}(z)} \{\mathbf{v}_{k-1}^\varepsilon(\text{next}^u(z))\}$.

Definition 3. The approximate optimal pattern of length k associated to $z \in \mathcal{X}$, denoted by $\pi_k^\varepsilon(z) \in U^k$, is defined by:

- if $k = 0$, $\pi_k^\varepsilon(z) = \text{nil}$,
- if $k \geq 1$, $\pi_k^\varepsilon(z) = \mathbf{u}_k(z) \cdot \pi'$ where

$$\mathbf{u}_k(z) = \arg \min_{u \in \text{Adm}(z) \subseteq U} \{\mathbf{v}_{k-1}^\varepsilon(\text{next}^u(z))\}$$

and $\pi' = \pi_{k-1}^\varepsilon(z')$ with $z' = \text{next}^{\mathbf{u}_k(z)}(z)$.

It is easy to construct a procedure $PROC_k^\varepsilon$ which takes a point $z \in \mathcal{X}$ as input, and returns an approximate optimal pattern $\pi_k^\varepsilon \in U^k$.

Remark 1. The complexity of $PROC_k^\varepsilon$ is $O(m \times k \times N)$ where m is the number of modes ($|U| = m$), k the time-horizon length ($t_{\text{end}} = k\tau$) and N the number of cells of \mathcal{X} ($N = K^M$).

2.3 Correctness of the method

Given a point $y \in S$ of ε -representative $z \in \mathcal{X}$, and a pattern π_k^ε returned by $PROC_k^\varepsilon(z)$, we are now going to show that the distance $\|\tilde{Y}_{k\tau,z}^{\pi_k^\varepsilon} - y_{\text{end}}\|$ converges to $\mathbf{v}_k(y)$ as $\varepsilon \rightarrow 0$. We first consider the ODE: $\frac{dy}{dt} = f_u(y)$, and give an upper bound to the error between the exact solution of the ODE and its Euler approximation (see [CF19b; Le +17b]).

Definition 4. Let μ be a given positive constant. Let us define, for all $u \in U$ and $t \in [0, \tau]$, $\delta_{t,\mu}^u$ as follows:

$$\text{if } \lambda_u < 0 : \quad \delta_{t,\mu}^u = \left(\mu^2 e^{\lambda_u t} + \frac{C_u^2}{\lambda_u^2} \left(t^2 + \frac{2t}{\lambda_u} + \frac{2}{\lambda_u^2} (1 - e^{\lambda_u t}) \right) \right)^{\frac{1}{2}}$$

$$\text{if } \lambda_u = 0 : \quad \delta_{t,\mu}^u = (\mu^2 e^t + C_u^2 (-t^2 - 2t + 2(e^t - 1)))^{\frac{1}{2}}$$

$$\text{if } \lambda_u > 0 : \quad \delta_{t,\mu}^u = \left(\mu^2 e^{3\lambda_u t} + \frac{C_u^2}{3\lambda_u^2} \left(-t^2 - \frac{2t}{3\lambda_u} + \frac{2}{9\lambda_u^2} (e^{3\lambda_u t} - 1) \right) \right)^{\frac{1}{2}}$$

where C_u and λ_u are real constants specific to function f_u , defined as follows:

$$C_u = \sup_{y \in S} L_u \|f_u(y)\|,$$

where L_u denotes the Lipschitz constant for f_u , and λ_u is the OSL constant associated to f_u , i.e., the minimal constant such that, for all $y_1, y_2 \in S$:

$$\langle f_u(y_1) - f_u(y_2), y_1 - y_2 \rangle \leq \lambda_u \|y_1 - y_2\|^2,$$

where $\langle \cdot, \cdot \rangle$ denotes the scalar product of two vectors of S .

Proposition 1. [Le +17b] Consider the solution Y_{t,y_0}^u of $\frac{dy}{dt} = f_u(y)$ with initial condition y_0 of ε -representative z_0 (hence such that $\|y_0 - z_0\| \leq \varepsilon$), and the approximate solution \tilde{Y}_{t,z_0}^u given by the explicit Euler scheme. For all $t \in [0, \tau]$, we have:

$$\|Y_{t,y_0}^u - \tilde{Y}_{t,z_0}^u\| \leq \delta_{t,\varepsilon}^u.$$

Proposition 1 underlies the principle of our set-based method where set of points are represented as balls centered around the Euler approximate values of the solutions. This is illustrated in Fig. 1: for any initial condition x^0 belonging to the ball $B(\tilde{x}^0, \delta(0))$, the exact solution $x^1 \equiv Y_{\tau, x^0}^u$ belongs to the ball $B(\tilde{x}^1, \delta(\tau))$ where $\tilde{x}^1 \equiv \tilde{Y}_{\tilde{x}^0, \tau}^u$ denotes the Euler approximation of the exact solution at $t = \tau$, and $\delta(\tau) \equiv \delta_{\tau, \delta(0)}^u$.

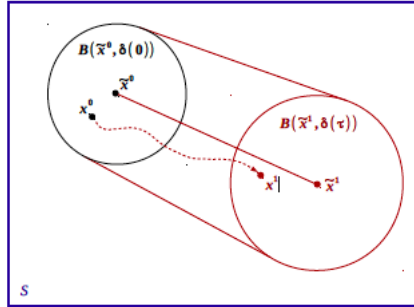


Fig. 1. Illustration of Proposition 1

Lemma 1. [CF19b] Consider the system $\frac{dy}{dt} = f_u(y)$ where the OSL constant λ_u associated to f_u is negative, and initial error $e_0 := \|y_0 - z_0\| > 0$. Let $G_u := \frac{\sqrt{3}e_0|\lambda_u|}{C_u}$. Consider the (smallest) positive root

$$\alpha_u := 1 + |\lambda_u|G_u/4 - \sqrt{1 + (\lambda_u G_u/4)^2}$$

of equation: $-\frac{1}{2}|\lambda_u|G_u + (2 + \frac{1}{2}|\lambda_u|G_u)\alpha - \alpha^2 = 0$.

Suppose: $\frac{|\lambda_u|G_u}{4} < 1$. Then we have $0 < \alpha_u < 1$, and, for all $t \in [0, \tau]$ with $\tau \leq G_u(1 - \alpha_u)$:

$$\delta_{e_0}^u(t) \leq e_0.$$

Remark 2. If $\tau > G_u(1 - \alpha_u)$, we can make use of *subsampling*, i.e., decompose τ into a sequence of elementary time steps Δt with $\Delta t \leq G_u(1 - \alpha_u)$ in order to be still able to apply [Lemma 1](#). Let us point out that [Lemma 1](#) (and the use of subsampling) allows to ensure set-based reachability with the use of procedure $PROC_k^\varepsilon$. Indeed, in this setting, the explicit Euler scheme leads to decreasing errors, and thus, point based computations performed with the center of a cell can be applied to the entire cell.

We suppose henceforth that, for all $u \in U$, the system $\frac{dy}{dt} = f_u(y)$ satisfies:

$$(H) : \quad \lambda_u < 0, \quad \frac{|\lambda_u|G_u}{4} < 1 \quad \text{and} \quad \tau \leq G_u(1 - \alpha_u), \quad \text{for all } u \in U.$$

We have:

Theorem 1. (*Convergence*) [[CF19b](#)]. Let $y \in S$ be a point of ε -representative $z \in \mathcal{X}$. Let π_k^ε be the pattern returned by $PROC_k^\varepsilon(z)$, and $\pi^* := \operatorname{argmin}_{\pi \in U_k} \|Y_{k\tau, y}^\pi - y_f\|$. Let $\mathbf{v}_k(y) := \|Y_{k\tau, y}^{\pi^*} - y_{end}\|$ be the exact optimal value of y . The approximate optimal value of y , $\|\tilde{Y}_{k\tau, y}^{\pi_k^\varepsilon} - y_{end}\|$, converges to $\mathbf{v}_k(y)$ as $\varepsilon \rightarrow 0$.

[Theorem 1](#) formally justifies the correctness of our method of optimal control synthesis by saying that the approximate optimal values computed by our method converge to the exact optimal values when the mesh size tends to 0. Furthermore, we have:

Theorem 2. (*Robustness*) [[CF19b](#)]. Let $y \in S$ be a point of ε -representative $z \in \mathcal{X}$, and π_k^ε the pattern returned by $PROC_k^\varepsilon(z)$. We have:

$$\|Y_{t, y}^\pi - \tilde{Y}_{t, z}^\pi\| \leq \varepsilon, \quad \text{for all } \pi \in U^k \text{ and } t \in [0, k\tau].$$

It follows that, for two points $y_1, y_2 \in S$ having the same ε -representative $z \in \mathcal{X}$, we have:

$$\|\|\tilde{Y}_{k\tau, y_1}^{\pi_k^\varepsilon} - y_{end}\| - \|\tilde{Y}_{k\tau, y_2}^{\pi_k^\varepsilon} - y_{end}\|\| \leq \varepsilon.$$

Last inequality of [Theorem 2](#) says that the approximate optimal values of y_1 and y_2 are equal up to ε . This reflects the *robustness* of our method of optimal control synthesis against *uncertainties on initial conditions*. As for uncertainties on initial conditions, one has similar robustness results accounting for dynamical *bounded disturbances*, as explained in [Appendix A](#).

2.4 Implementation

The implementation of the robust and variant methods has been done in Python. Each method corresponds to a program of around 500 lines. The source code is available at lipn.univ-paris13.fr/~jerry/synchro/. In the experiments below, the program runs on a 2.80 GHz Intel Core i7-4810MQ CPU with 8 GiB of memory.

2.5 Example: Magnetic Resonance Imaging (MRI)

Considering a system q consisting of two different particles with spins q_1, q_2 (see [Bon+13; Bon+14]). The magnetization vectors $q_1 = (y_1, z_1) \in \mathbb{R}^2$ and $q_2 = (y_2, z_2) \in \mathbb{R}^2$ satisfy the differential system:

$$q_1 : \begin{cases} \dot{y}_1 = 2\pi T_m t_m (-\Gamma_1 y_1 - u_2 z_1) \\ \dot{z}_1 = 2\pi T_m t_m (\gamma_1 (1 - z_1) + u_2 y_1) \end{cases}$$

$$q_2 : \begin{cases} \dot{y}_2 = 2\pi T_m t_m (-\Gamma_2 y_2 - u_2 z_2) \\ \dot{z}_2 = 2\pi T_m t_m (\gamma_2 (1 - z_2) + u_2 y_2) \end{cases}$$

with: $\Gamma_1 = \frac{1}{T_{12}\Omega_{max}}$, $\gamma_1 = \frac{1}{T_{11}\Omega_{max}}$, $\Gamma_2 = \frac{1}{T_{22}\Omega_{max}}$, $\gamma_2 = \frac{1}{T_{21}\Omega_{max}}$, and $u_2 \in [-1, 1]$ the magnetic field (control). Let $\Omega_{max} = 202.95$, $T_{11} = 2$, $T_{12} = 0.3$, $T_{21} = 2.5$, $T_{22} = 2.5$, $T_m = 26.17$ and $t_m = 2$. The goal is to make q_1 reach the origin $(0, 0)$ at a given time $t = t_{end}$ while maximizing the ‘‘contrast’’ $\|q_2(t_{end}) - q_1(t_{end})\| = \|q_2(t_{end})\|$. In order to account for the (soft) constraint $q_1(t_{end}) = (0, 0)$, we integrate in the cost function J_k a ‘‘penalty term’’ of the form $\|q_1(t_{end})\|^2$. Our goal is thus to minimize the terminal cost: $\alpha\|q_1(t_{end})\|^2 - \beta\|q_2(t_{end}) - q_1(t_{end})\|^2$. The domain S of the states $(q_1, q_2) \equiv ((y_1, z_1), (y_2, z_2))$ is equal to $[-1, 1]^2 \times [-1, 1]^2 \equiv [-1, 1]^4$. The grid \mathcal{X} corresponds to a discretization of $S = [-1, 1]^4$, where each component interval $[-1, 1]$ is uniformly discretized into a set of K points. The codomain $[-1, 1]$ of the original continuous control function $u_2(\cdot)$ is itself discretized into a finite set U with our method. After discretization, $u_2(\cdot)$ is a piecewise-constant function that takes its values in the finite set U made of 30 values uniformly taken between -1 and 1 . The function $u_2(\cdot)$ can change its value every τ seconds. In the following experiments, we use the following parameter values: $\alpha = 0.99$, $\beta = 0.01$, $\tau = 1/250$, $k = 215$, $t_{end} = k\tau = 0.86$, and $q_1(0) = (0, 1)$. We will consider the cases $K = 10$ (coarse grid) and $K = 20$ (finer grid). One can check that assumption (H) is satisfied in both cases. In order to test the robustness of the method, we will consider the cases $q_2(0) = (0, 1)$ and $q_2(0) = (0.1, 1)$.

For $K = 10$ and $q_2(0) = (0, 1)$, we have $q_2(t_{end}) = (0.6567, -0.2558)$, and the optimal value of the contrast is $\|q_2(t_{end})\| = 0.7048$. The CPU computation takes 389 seconds. See Fig. 2. For $q_2(0) = (0.1, 1)$, the synthesized control and the results are identical, which demonstrates the robustness of our method.

For $K = 20$, and $q_2(0) = (0, 1)$, we have $q_2(t_{end}) = (0.6439, -0.2913)$, and the contrast is $\|q_2(t_{end})\| = 0.7067$. (see Fig. 3). The CPU computation takes 3657 seconds. See Fig. 3. For $q_2(0) = (0.1, 1)$, the synthesized control and the results are again identical, thus confirming the robustness of our method.

For comparison, we now perform the same experiments with the version of the numerical solver Bocop using convex optimization [Tea17]. For $q_2(0) = (0, 1)$, we have with Bocop: $q_2(t_{end}) = (0.0499, -0.7938)$; the contrast is $\|q_2(t_{end})\| = 0.6746$. The CPU computation time is 230 seconds. See Fig. 6 (Appendix B). For $q_2(0) = (0.1, 1)$, we have, with Bocop: $q_2(t_{end}) = (0.0877, -0.6631)$; the contrast is $\|q_2(t_{end})\| = 0.6689$. The CPU computation time is 43 seconds. See Fig. 7

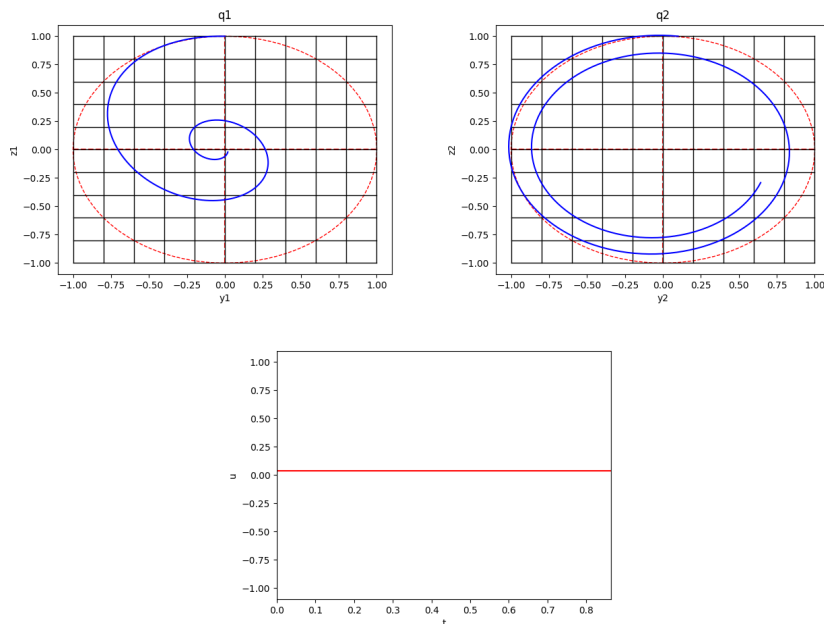


Fig. 2. Robust method applied to MRI for $K = 10$ and initial condition $q_2(0) = (0.1, 1)$, with $q_1 = (y_1, z_1)$ (top left), $q_2 = (y_2, z_2)$ (top right) and control u_2 (bottom). When applied to $q_2(0) = (0, 1)$, the method gives the same results.

(Appendix B). We can see on this example that Bocop is *not* robust against slight changes of initial conditions, the generated optimal trajectories being very different from each other. The optimal values of the contrast computed by Bocop and our program are comparable. However, the CPU times of Bocop are smaller than those of our program (especially for $K = 20$).

3 A Variant of the Method with Receding Horizon

The control computed by our method is robust, but its synthesis is time-costly because it requires a fine partition of the state space in order to decrease the error caused by the space discretization. We are now considering a variant of our method, inspired by the Model Predictive Control Method (MPC) which uses a *receding horizon* [May14]. In the original method, for a k -horizon problem ($t_{end} = k\tau$), to a point $y \in S$ is applied the optimal pattern $\pi(z)$ of length k computed for the ε -representative z of y (returned by $PROC_k^\varepsilon(z)$). In the variant inspired by MPC, we apply at point y only the first mode u_1 of $\pi(z)$, thus obtaining the point $y_1 = y + \tau f_{u_1}(y)$. Then, unlike the original method, we do not apply the second mode u_2 of $\pi(z)$, but we apply the first mode u'_1 of the optimal pattern $\pi(z_1)$ (returned by $PROC_k^\varepsilon(z_1)$), where z_1 denotes the

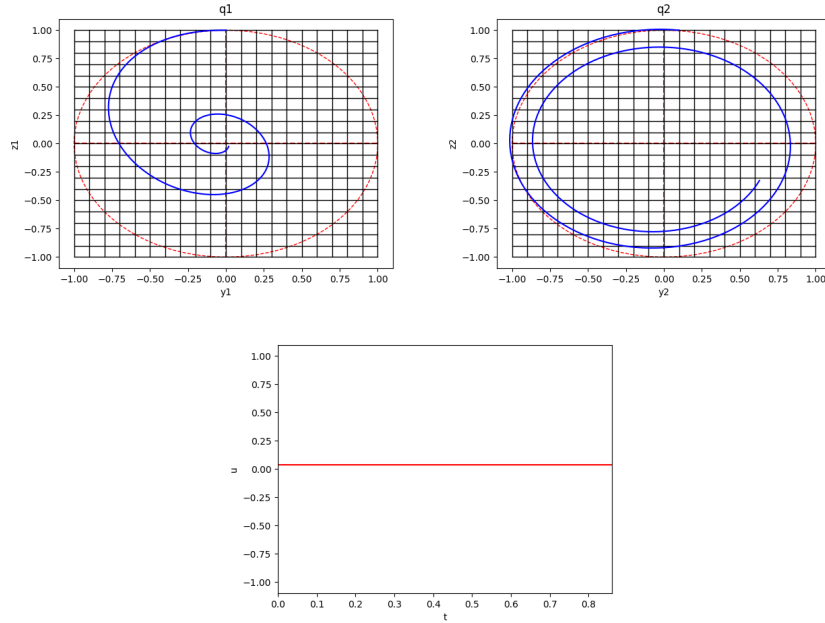


Fig. 3. Robust method applied to MRI for $K = 20$ and initial condition $q_2(0) = (0.1, 1)$, with $q_1 = (y_1, z_1)$ (top left), $q_2 = (y_2, z_2)$ (top right) and control u_2 (bottom). When applied to $q_2(0) = (0, 1)$, the method gives the same results.

ε -representative of y_1 . This gives $y_2 = y_1 + \tau f_{u'_1}(y_1)$ (and not $y_1 + \tau f_{u_2}(y_1)$ as before). And so on, iteratively, one applies each time the first mode of the optimal pattern $\pi(z_n)$ returned by $PROC_k^\varepsilon(z_n)$, where z_n denotes the ε -representative of the solution y_n computed at $t = n\tau$ ($1 \leq n \leq k - 1$).

This variant is not any longer robust: trajectories from two close starting points do not usually stay close to each other anymore. On the other hand, the computed values converge much faster to the exact optimal values as ε tends to 0. This allows us to compute values of similar precision with the variant method, using a much coarser grid (bigger ε). The variant method is therefore more efficient than the original method. We demonstrate this gain of efficiency and loss of robustness on the MRI example of [Section 2.5](#). We first synthesize the optimal control for $K = 10$ and $q_2(0) = (0, 1)$, in which case we have: $q_2(t_{end}) = (0.0499, -0.7938)$, and the contrast is $\|q_2(t_{end})\| = 0.7954$. (see [Fig. 4](#)). For $K = 10$ and $q_2(0) = (0.1, 1)$, we have: $q_2(t_{end}) = (0.1015, -0.7141)$, and the contrast $\|q_2(t_{end})\|$ is 0.7210. (see [Fig. 5](#)). For both cases, the CPU computation takes 34 seconds. We can see on this example that, unlike the original method, the variant method is *not* robust, a small difference between the initial conditions ($q_2(0) = (0, 1)$ vs. $q_2(0) = (0.1, 1)$) leading to very different trajectories.

For $K = 20$ and $q_2(0) = (0, 1)$, we have $q_2(t_{end}) = (-0.06225, -0.5874)$, and the contrast $\|q_2(t_{end})\|$ is 0.5906. (see Fig. 8 in Appendix C). The CPU computation now takes 443 seconds. For $K = 20$ and $q_2(0) = (0.1, 1)$, we have $q_2(t_{end}) = (-0.1088, -0.7192)$, and the contrast $\|q_2(t_{end})\|$ is 0.7274. (see Fig. 9 in Appendix C). The CPU computation now takes 501 seconds.

On the MRI example, the CPU times of the variant method are thus much smaller than those of the original method, and comparable to those of Bocop. Besides, the optimal values of the contrast computed by the variant method are slightly better than those computed by Bocop. The variant method is thus more efficient than the original method, but does not retain its robustness property. There is therefore a trade-off to be found between robustness (guaranteed with the original method) and efficiency (obtained with the MPC variant).

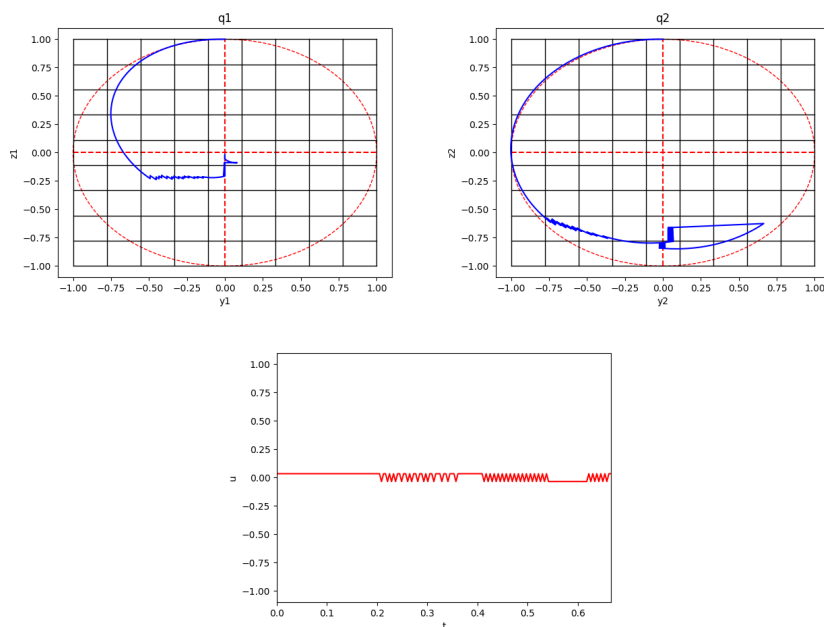


Fig. 4. Variant with receding horizon applied to MRI for initial condition $q_2(0) = (0, 1)$, with $q_1 = (y_1, z_1)$ (top left), $q_2 = (y_2, z_2)$ (top right) and control u_2 (bottom).

The results of Sections 2 and 3 for $x_2(0) = (0.1, 1)$ are recapitulated in Table 1.

4 Conclusion

As pointed out in [Hey+18; Tea17], numerical methods of optimal control, based on DPP, can compete on low dimensional examples, with methods based on

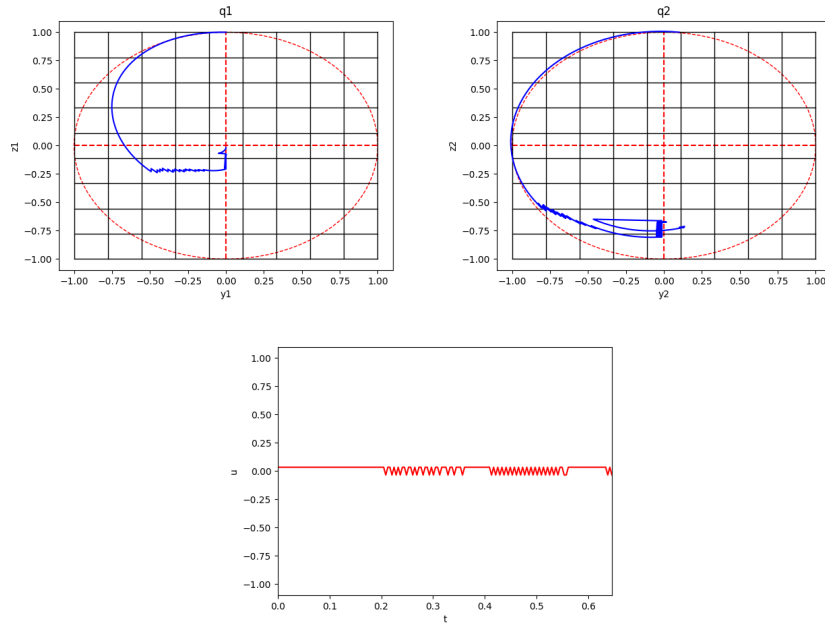


Fig. 5. Variant with receding horizon applied to MRI for initial condition $q_2(0) = (0.1, 1)$, with $q_1 = (y_1, z_1)$ (top left), $q_2 = (y_2, z_2)$ (top right) and control u_2 (bottom).

	robust method(K=10)	robust method(K=20)	variant(K=10)	variant(K=20)	Bocop
Robust?	yes	yes	no	no	no
Contrast:	0.7048	0.7669	0.7210	0.7273	0.6746
CPU time (s):	389	3657	34	501	230

Table 1. Summary table of results

convex optimization. Along these lines, we show in this paper that a set-based method of optimal control combining DPP and a guaranteed Euler integration method, allows to synthesize a correct-by-design optimal control that is *robust* against uncertainties on initial conditions and bounded disturbances. We have demonstrated the practical interest of our method on an example taken from the numerical Bocop solver. We have observed similar results in experiments with other case studies from Bocop, that will be given in the extended version of this paper. We have also considered a variant of our method with a receding horizon, that makes the control synthesis more efficient at the cost of losing the robustness property. There is therefore a trade-off to be found between robustness (guaranteed with the original method) and efficiency (obtained with the variant using a receding horizon).

References

- [ASB07] Matthias Althoff, Olaf Stursberg, and Martin Buss. “Reachability analysis of linear systems with uncertain parameters and inputs”. In: *CDC*. (Dec. 12–14, 2007). New Orleans, LA, USA, 2007, pp. 726–732. DOI: [10.1109/CDC.2007.4434084](https://doi.org/10.1109/CDC.2007.4434084) (cit. on p. 2).
- [Bel57] Richard Bellman. *Dynamic Programming*. 1st ed. Princeton, NJ, USA: Princeton University Press, 1957 (cit. on p. 2).
- [BH98] Martin Berz and Georg Hoffstätter. “Computation and Application of Taylor Polynomials with Interval Remainder Bounds”. In: *Reliable Computing* 4.1 (1998), pp. 83–97. DOI: [10.1023/A:1009958918582](https://doi.org/10.1023/A:1009958918582) (cit. on p. 2).
- [BM98] Martin Berz and Kyoko Makino. “Verified Integration of ODEs and Flows Using Differential Algebraic Methods on High-Order Taylor Models”. In: *Reliable Computing* 4.4 (1998), pp. 361–369. DOI: [10.1023/A:1024467732637](https://doi.org/10.1023/A:1024467732637) (cit. on p. 2).
- [BMG12] Frédéric Bonnans, Pierre Martinon, and Vincent Grélard. *Bocop – A collection of examples*. Tech. rep. RR-8053. <https://hal.inria.fr/hal-00726992>. INRIA, 2012 (cit. on p. 2).
- [Bon+13] Bernard Bonnard, Mathieu Claeys, Olivier Cots, and Pierre Martinon. “Comparison of Numerical Methods in the Contrast Imaging Problem in NMR”. In: *CDC*. (Dec. 10–13, 2013). Firenze, Italy: IEEE, Dec. 2013, pp. 4523–4528. DOI: [10.1109/CDC.2013.6760586](https://doi.org/10.1109/CDC.2013.6760586) (cit. on p. 8).
- [Bon+14] Bernard Bonnard, Mathieu Claeys, Olivier Cots, and Pierre Martinon. “Geometric and Numerical Methods in the Contrast Imaging Problem in Nuclear Magnetic Resonance”. In: *Acta Applicandae Mathematicae* 135 (Feb. 2014), pp. 5–45. DOI: [10.1007/s10440-014-9947-3](https://doi.org/10.1007/s10440-014-9947-3) (cit. on p. 8).
- [CAS12] Xin Chen, Erika Abraham, and Sriram Sankaranarayanan. “Taylor Model Flowpipe Construction for Non-linear Hybrid Systems”. In: *RTSS*. (Dec. 4–7, 2012). San Juan, PR, USA: IEEE Computer Society, 2012, pp. 183–192. DOI: [10.1109/RTSS.2012.70](https://doi.org/10.1109/RTSS.2012.70) (cit. on p. 2).
- [CF19a] Adrien Le Coënt and Laurent Fribourg. “Guaranteed Control of Sampled Switched Systems using Semi-Lagrangian Schemes and One-Sided Lipschitz Constants”. In: *CDC*. (Dec. 11–13, 2019). Nice, France: IEEE, 2019, pp. 599–604. DOI: [10.1109/CDC40024.2019.9029376](https://doi.org/10.1109/CDC40024.2019.9029376) (cit. on pp. 2, 4).
- [CF19b] Adrien Le Coënt and Laurent Fribourg. “Guaranteed Optimal Reachability Control of Reaction-Diffusion Equations Using One-Sided Lipschitz Constants and Model Reduction”. In: *WESE*. (Oct. 17–18, 2019). Ed. by Roger D. Chamberlain, Martin Grimheden, and Walid Taha. Vol. 11971. LNCS. New York City, NY, USA: Springer, 2019, pp. 181–202. DOI: [10.1007/978-3-030-41131-2_9](https://doi.org/10.1007/978-3-030-41131-2_9) (cit. on pp. 2, 4–7).
- [FG99] Maurizio Falcone and Tiziana Giorgi. “An Approximation Scheme for Evolutive Hamilton-Jacobi Equations”. In: *Stochastic Analysis, Control, Optimization and Applications: A Volume in Honor of W.H. Fleming*. Boston, MA: Birkhäuser Boston, 1999, pp. 289–303. ISBN: 978-1-4612-1784-8. DOI: [10.1007/978-1-4612-1784-8_17](https://doi.org/10.1007/978-1-4612-1784-8_17) (cit. on p. 2).
- [Gir05] Antoine Girard. “Reachability of uncertain linear systems using zonotopes”. In: *HSCC*. Ed. by Manfred Morari and Lothar Thiele. Vol. 3414. LNCS. Zürich, Switzerland: Springer, 2005, pp. 291–305. DOI: [10.1007/978-3-540-31954-2_19](https://doi.org/10.1007/978-3-540-31954-2_19) (cit. on p. 2).

- [Hey+18] Benjamin Heymann, J. Frédéric Bonnans, Pierre Martinon, Francisco J. Silva, Fernando Lanas, and Guillermo Jiménez-Estévez. “Continuous optimal control approaches to microgrid energy management”. In: *Energy Systems* 9.1 (2018), pp. 59–77. DOI: [10.1007/s12667-016-0228-2](https://doi.org/10.1007/s12667-016-0228-2) (cit. on pp. 2, 11).
- [HK06] Zhi Han and Bruce H. Krogh. “Reachability Analysis of Large-Scale Affine Systems Using Low-Dimensional Polytopes”. In: *HSCC*. (Mar. 29–31, 2006). Santa Barbara, CA, USA, 2006, pp. 287–301. DOI: [10.1007/11730637_23](https://doi.org/10.1007/11730637_23) (cit. on p. 2).
- [Kir70] Donald E Kirk. *Optimal control theory: an introduction*. Springer, 1970 (cit. on p. 2).
- [Le +17a] Adrien Le Coënt, Julien Alexandre Dit Sandretto, Alexandre Chapoutot, Laurent Fribourg, Florian De Vuyst, and Ludovic Chamoin. “Distributed Control Synthesis using Euler’s Method”. In: *RP*. (Sept. 7–9, 2017). Ed. by Matthew Hague and Igor Potapov. Vol. 247. LNCS. London, UK: Springer, 2017, pp. 118–131. DOI: [10.1007/978-3-319-67089-8_9](https://doi.org/10.1007/978-3-319-67089-8_9) (cit. on p. 16).
- [Le +17b] Adrien Le Coënt, Florian De Vuyst, Ludovic Chamoin, and Laurent Fribourg. “Control Synthesis of Nonlinear Sampled Switched Systems using Euler’s Method”. In: *SNR*. (Apr. 22, 2017). Ed. by Erika Ábrahám and Sergiy Bogomolov. Vol. 247. EPTCS. Uppsala, Sweden, 2017, pp. 18–33. DOI: [10.4204/EPTCS.247.2](https://doi.org/10.4204/EPTCS.247.2) (cit. on pp. 2, 5, 6).
- [Loh87] Rudolf J. Lohner. “Enclosing the solutions of ordinary initial and boundary value problems”. In: *Computer Arithmetic* (1987), pp. 255–286 (cit. on p. 2).
- [LTS99] John Lygeros, Claire Tomlin, and Shankar Sastry. “Controllers for reachability specifications for hybrid systems”. In: *Automatica* 35.3 (1999), pp. 349–370. DOI: [10.1016/S0005-1098\(98\)00193-9](https://doi.org/10.1016/S0005-1098(98)00193-9) (cit. on p. 2).
- [May14] David Q. Mayne. “Model predictive control: Recent developments and future promise”. In: *Automatica* 50.12 (2014), pp. 2967–2986. DOI: [10.1016/j.automatica.2014.10.128](https://doi.org/10.1016/j.automatica.2014.10.128) (cit. on pp. 1, 2, 9).
- [MBT01] Ian M. Mitchell, Alexandre M. Bayen, and Claire J. Tomlin. “Validating a Hamilton-Jacobi Approximation to Hybrid System Reachable Sets”. In: *HSCC*. (Mar. 28–30, 2001). Rome, Italy, 2001, pp. 418–432. DOI: [10.1007/3-540-45351-2_34](https://doi.org/10.1007/3-540-45351-2_34) (cit. on p. 2).
- [Moo66] Ramon Moore. *Interval Analysis*. Prentice Hall, 1966 (cit. on p. 2).
- [MSR05] David Q. Mayne, Mariéa M. Seron, and Sasa V. Rakovic. “Robust model predictive control of constrained linear systems with bounded disturbances”. In: *Automatica* 41.2 (2005), pp. 219–224. DOI: [10.1016/j.automatica.2004.08.019](https://doi.org/10.1016/j.automatica.2004.08.019) (cit. on p. 2).
- [MT03] Ian M. Mitchell and Claire Tomlin. “Overapproximating Reachable Sets by Hamilton-Jacobi Projections”. In: *Journal of Scientific Computing* 19.1-3 (2003), pp. 323–346. DOI: [10.1023/A:1025364227563](https://doi.org/10.1023/A:1025364227563) (cit. on p. 2).
- [Neu93] A. Neumaier. “The Wrapping Effect, Ellipsoid Arithmetic, Stability and Confidence Regions”. In: *Computing Supplementum*. Vienna: Springer Vienna, 1993, pp. 175–190 (cit. on p. 2).
- [NJC99] Nedialko S. Nedialkov, K. Jackson, and Georges Corliss. “Validated solutions of initial value problems for ordinary differential equations”. In: *Applied Mathematics and Computation* 105.1 (1999), pp. 21–68. DOI: [10.1016/S0096-3003\(98\)10083-8](https://doi.org/10.1016/S0096-3003(98)10083-8) (cit. on p. 2).

- [NKS04] Nedialko S. Nedialkov, Vladik Kreinovich, and Scott A. Starks. “Interval arithmetic, affine arithmetic, Taylor series methods: Why, what next?” In: *Numerical Algorithms* 37.1-4 (2004), pp. 325–336. DOI: [10.1023/B:NUMA.0000049478.42605.cf](https://doi.org/10.1023/B:NUMA.0000049478.42605.cf) (cit. on p. 2).
- [NN94] Yurii E. Nesterov and Arkadii Nemirovskii. *Interior-point polynomial algorithms in convex programming*. Vol. 13. Siam studies in applied mathematics. SIAM, 1994. ISBN: 978-0-89871-319-0. DOI: [10.1137/1.9781611970791](https://doi.org/10.1137/1.9781611970791) (cit. on p. 1).
- [RR19] Gunther Reissig and Matthias Rungger. “Symbolic Optimal Control”. In: *IEEE Transactions on Automatic Control* 64.6 (2019), pp. 2224–2239. DOI: [10.1109/TAC.2018.2863178](https://doi.org/10.1109/TAC.2018.2863178) (cit. on p. 2).
- [SA17a] Bastian Schürmann and Matthias Althoff. “Guaranteeing Constraints of Disturbed Nonlinear Systems Using Set-Based Optimal Control in Generator Space”. In: *IFAC-PapersOnLine* 50.1 (2017). 20th IFAC World Congress, pp. 11515–11522. ISSN: 2405-8963. DOI: <https://doi.org/10.1016/j.ifacol.2017.08.1617> (cit. on pp. 2, 16).
- [SA17b] Bastian Schürmann and Matthias Althoff. “Optimal control of sets of solutions to formally guarantee constraints of disturbed linear systems”. In: *ACC*. (May 24–26, 2017). Seattle, WA, USA, 2017, pp. 2522–2529. DOI: [10.23919/ACC.2017.7963332](https://doi.org/10.23919/ACC.2017.7963332) (cit. on p. 2).
- [SAF18] Luca Saluzzi, Alessandro Alla, and Maurizio Falcone. *Error estimates for a tree structure algorithm solving finite horizon control problems*. 1812.11194. 2018. arXiv: [1812.11194](https://arxiv.org/abs/1812.11194) (cit. on p. 2).
- [SKA18] Bastian Schürmann, Niklas Kochdumper, and Matthias Althoff. “Reach-set Model Predictive Control for Disturbed Nonlinear Systems”. In: *CDC*. (Dec. 17–19, 2018). Miami, FL, USA, 2018, pp. 3463–3470. DOI: [10.1109/CDC.2018.8619781](https://doi.org/10.1109/CDC.2018.8619781) (cit. on p. 2).
- [Tea17] Inria Saclay Team Commands. *BOCOP: an open source toolbox for optimal control*. <http://bocop.org>. 2017 (cit. on pp. 2, 8, 11).

A Robustness against bounded disturbances

A differential system with “bounded disturbances” is of the form

$$\frac{dy(t)}{dt} = f_u(y(t), w(t)),$$

with $u \in U$, $t \in [0, \tau]$, states $y(t) \in \mathbb{R}^M$, and disturbances $w(t) \in \mathcal{W} \subset \mathbb{R}^d$ (\mathcal{W} is compact, i.e., closed and bounded). See, e.g., [SA17a]. We assume that any possible disturbance trajectory is bounded in the compact set \mathcal{W} for $t \in [0, \tau]$. We use $\phi_u(t; y^0, w(\cdot))$ to denote the solution of $\frac{dy(t)}{dt} = f_u(y(t), w(t))$ for $t \in [0, \tau]$ with $y(0) = y^0$. If we consider an undisturbed system, we use $\phi_u(t; y^0, 0)$ (resp. $\tilde{\phi}_u(t; y^0, 0)$) to denote the solution (resp. the approximate Euler solution) without disturbances, i.e., $\mathcal{W} = 0$.

Given a pattern $\pi = u_k \cdots u_1 \in U^k$, these notations extend naturally to $t \in [0, k\tau]$ by considering the solutions obtained by applying successive modes u_k, \dots, u_1 in a continuous manner. The optimization task is now to find a control pattern $\pi \in U^k$ which guarantees that all states in $S \subset \mathbb{R}^M$ are steered at time $t = k\tau$ as closely as possible to an end state y_{end} , *despite the disturbance set* \mathcal{W} .

We now suppose that S is controlled Euler-invariant for the *undisturbed* system, i.e.: for all $y \in S$, there exists u such that $\tilde{\phi}_u(\tau; y, 0) \in S$.

We also suppose (see [Le +17a]) that, for all $u \in U$, there exist constants $\lambda_u \in \mathbb{R}_{<0}$ and $\gamma_u \in \mathbb{R}_{\geq 0}$ such that, for all $y_1, y_2 \in S$ and $w_1, w_2 \in \mathcal{W}$:

$$\langle f_u(y_1, w_1) - f_u(y_2, w_2), y_1 - y_2 \rangle \leq \lambda_u \|y_1 - y_2\|^2 + \gamma_u \|y_1 - y_2\| \|w_1 - w_2\| \quad (H1).$$

We now give a version of [Proposition 1](#) with bounded disturbance $w(\cdot) \in \mathcal{W}$.

Proposition 2. [Le +17a] *Given a sampled switched system with bounded disturbance of the form $\{\frac{dy(t)}{dt} = f_u(y(t), w(t))\}_{u \in U}$ satisfying (H1) for all $u \in U$, consider a point $y_0 \in S$ of ε -representative $z^0 \in \mathcal{X}$. We have, for all $w(\cdot) \in \mathcal{W}$, $u \in U$:*

$$\|\phi_u(\tau; y^0, w(\tau)) - \tilde{\phi}_u(\tau; z^0, 0)\| \leq \delta_{\tau, \varepsilon, \mathcal{W}}^u.$$

with

$$\begin{aligned} \delta_{t, \varepsilon, \mathcal{W}}^u = & \left(\frac{C_u^2}{-\lambda_u^4} (-\lambda_u^2 t^2 - 2\lambda_u t + 2e^{\lambda_u t} - 2) \right. \\ & + \frac{1}{\lambda_u^2} \left(\frac{C_u \gamma_u |\mathcal{W}|}{-\lambda_u} (-\lambda_u t + e^{\lambda_u t} - 1) \right. \\ & \left. \left. + \lambda_u \left(\frac{\gamma_u^2 (|\mathcal{W}|/2)^2}{-\lambda_u} (e^{\lambda_u t} - 1) + \lambda_u \varepsilon^2 e^{\lambda_u t} \right) \right) \right)^{1/2} \quad (1) \end{aligned}$$

[Theorems 1](#) and [2](#) can themselves be extended to account for bounded disturbance $w(\cdot) \in \mathcal{W}$. The details will be given in the extended version of this paper.

B Sensitivity of Bocop to Initial Conditions

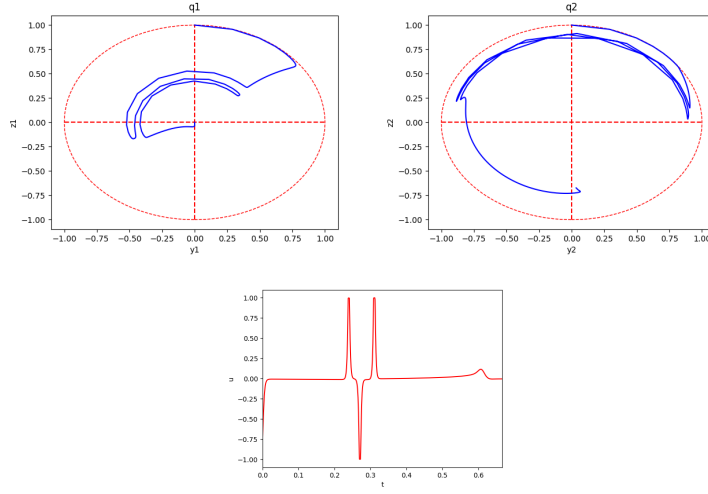


Fig. 6. Bocop solution on MRI when initially $q_2(0) = (0, 1)$, with $q_1 = (y_1, z_1)$ (top left), $q_2 = (y_2, z_2)$ (top right) and control u_2 (bottom).

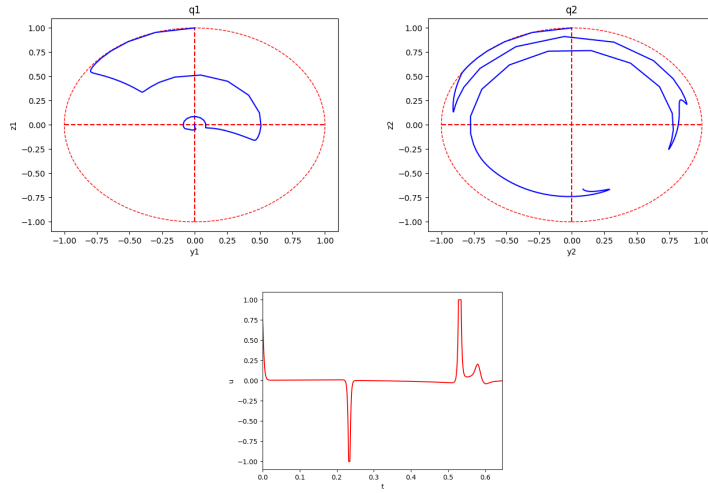


Fig. 7. Bocop solution on MRI for initial condition $q_2(0) = (0.1, 1)$, with $q_1 = (y_1, z_1)$ (top left), $q_2 = (y_2, z_2)$ (top right) and control u_2 (bottom).

C Results of variant with receding horizon applied to MRI with $K = 20$

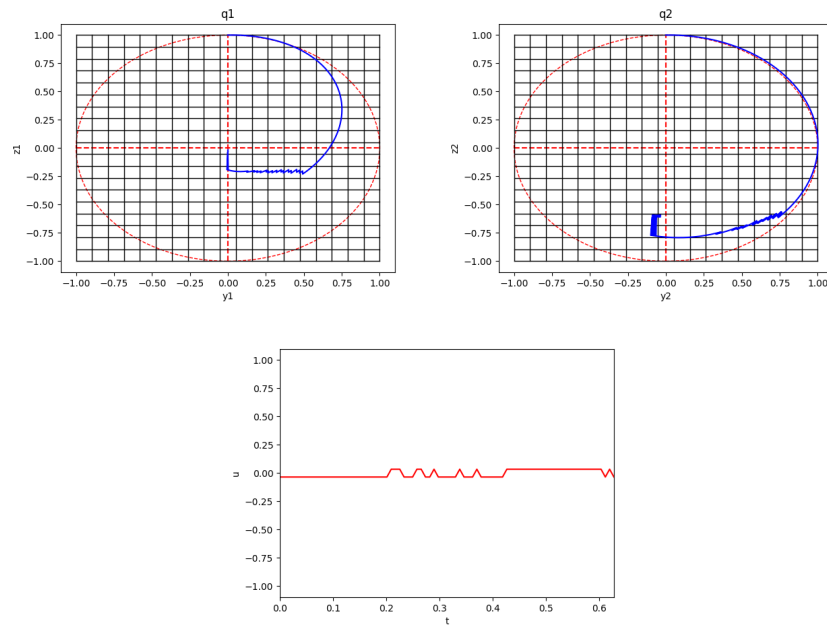


Fig. 8. Variant with receding horizon applied to MRI with a finer grid ($K = 20$) for initial condition $q_2(0) = (0, 1)$, with $q_1 = (y_1, z_1)$ (top left), $q_2 = (y_2, z_2)$ (top right) and control u_2 (bottom).

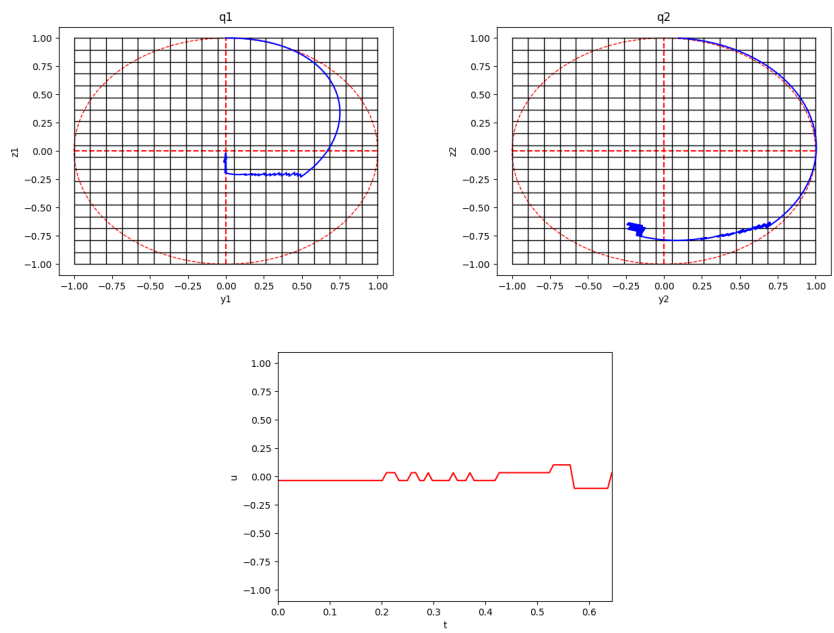


Fig. 9. Variant with receding horizon applied to MRI with a finer grid ($K = 20$) for initial condition $q_2(0) = (0.1, 1)$, with $q_1 = (y_1, z_1)$ (top left), $q_2 = (y_2, z_2)$ (top right) and control u_2 (bottom).